Food Chemistry: X 16 (2022) 100455

Contents lists available at ScienceDirect

Food Chemistry: X

journal homepage: www.sciencedirect.com/journal/food-chemistry-x

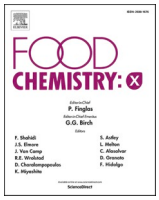

# Formation, structure and stability of high internal phase Pickering emulsions stabilized by BSPI-C3G covalent complexes

Xiaojie Cui [a,b,1], Mengyao Ma [a,b,1], Yanli Xie [a,b,*], Yuhui Yang [a,b], Qian Li [a,b], Shumin Sun [a,b], Weibin Ma [a,b]

[a] College of Food Science and Engineering, Henan University of Technology, Zhengzhou 450001, People's Republic of China
[b] Henan Key Laboratory of Cereal and Oil Food Safety Inspection and Control, Zhengzhou 450001, People's Republic of China

ARTICLE INFO

*Keywords:*
High internal phase Pickering emulsion
Stability
Lipid oxidation
Black soybean protein isolate
Cyanidin-3-O-glucoside

ABSTRACT

Food-grade high internal phase Pickering emulsions (HIPPEs) are stabilized by protein-based particles, which have attracted extensive attention due to their good gel-like structure. The black soybean isolate protein/cyanidin-3-O-glucoside (BSPI-C3G) covalent particles were used as a particulate emulsifier to form stable HIPPEs with oil phase fractions (74 % v/v) and low particle concentrations (0.5 %–3 % w/v) The particle size distribution and microstructure demonstrated that the BSPI-C3G covalent particles acted as an interfacial layer and surrounded the oil droplets. As the concentration of BSPI-C3G particles increased from 0.5 % to 3 %, the droplet size, elasticity, antioxidant capacity of the heated or stored HIPPEs more stable. So, the HIPPEs had the best stability with the BSPI-C3G particle at 3 % (w/v) concentration. These findings may extend the application of BSPI and C3G in foods and provide the guidelines for the rational design of food-grade HIPPEs stabilized by protein/anthocyanin complexes.

## 1. Introduction

Anthocyanins belong to the group of flavonoids and are vital secondary metabolites for fruit and vegetables (Li et al., 2019). They showed various colors at different pH and were the major color-presenting substances of plants, with strong antioxidant, anti-diabetic, anti-proliferative properties, and anti-inflammatory functions (Ma, Xie, & Wang, 2021). The antioxidant capacity of polyphenols directly relates to the hydroxyl group, which donates hydrogen, scavenges singlet oxygen and various types of free radicals, and chelates metal ions (Fu, Wang, Belwal, Xu, Li, & Luo, 2021). Black beans belong to the same family as soybeans, whose coat black color is due to the richness of anthocyanins such as cyanidin, delphinidin, petunidin, and pelargonidin as 3-O-glucosides, of which cyanidin-3-O-glucoside (C3G) is the most abundantly found anthocyanin (Chen et al., 2019). Despite the multiple health-promoting properties of anthocyanins from black soybeans, there was less research on black soybean anthocyanins than on berry anthocyanin.

Anthocyanins are not stable in nature, but the interaction of proteins and polyphenols occurs in food systems and can protect the stability of anthocyanins, alter the structural, functional, and nutritional properties of proteins and improve the stability of complexes (Li et al., 2021). Protein-anthocyanin complexes were formed by covalent and non-covalent bonds, such as hydrogen bonds, hydrophobic interactions, static quenching, and disulfide bonds (Fu, Belwal, He, Xu, Li, & Luo, 2020; Ma, Cheng, Jiao, & Jing, 2022). It was reported that preheated soybean isolate protein (SPI) could interact with black rice extract, and C3G through hydrophobic interactions or static quenching mechanisms. They reported that the following complex of SPI-anthocyanins, the digestibility, emulsifying, and foaming capabilities of SPI were improved as well as the thermal and oxidative stability of anthocyanins (Chen et al., 2019; Sui, Sun, Qi, Zhang, Li, & Jiang, 2018). There are some studies on the covalent complexes of SPI with black rice extract or C3G, and the stability of the complexes was improved (Ju et al., 2020; Sui et al., 2018). Generally, covalent complexes exhibited better foam and emulsion stability than non-covalent complexes. In simulated gastrointestinal studies, SPI with C3G, the main anthocyanin monomer in mulberry anthocyanins (MA) was binned through hydrophobic interactions,

* Corresponding author at: College of Food Science and Engineering, Henan University of Technology, 100# Lianhua Street, High-tech Industrial Development Zone, Zhengzhou 450001, Henan, People's Republic of China.
*E-mail address:* ylxie@haut.edu.cn (Y. Xie).
[1] These authors contributed equally to this work.

https://doi.org/10.1016/j.fochx.2022.100455
Received 1 August 2022; Received in revised form 20 September 2022; Accepted 22 September 2022
Available online 23 September 2022

promoting protein digestibility by pepsin (Ma et al., 2022). Black soybean protein isolate (BSPI), like SPI, contains high-quality amino acids, thus BSPI-polyphenol complexes deserve to be studied extensively.

Solid particles (including nanoparticles and particulates), which were difficult to desorb down from the interface, can prepare stable Pickering emulsions, including ordinary Pickering Emulsion (PE) and High Internal Phase Pickering Emulsion (HIPPE) (Shi, Feng, Wang, & Adhikari, 2020). High internal phase emulsions (HIPEs) are emulsions with a volume fraction of dispersed phase more than 74 % and show solid-like characteristics. SPI can self-assemble into nanoparticles after heating and is used widely as a stabilizer for emulsions due to its amphiphilic nature (Sui et al., 2018). Anthocyanins and SPI can form stable complexes, resulting in a significant reduction in particle size, which led to the preparation of better external digestibility and more stable emulsions (Ju et al., 2020; Sui et al., 2018). Pickering emulsions Stabilized by Gliadin/Proanthocyanidins Hybrid Particles (GPHPs) were found to delay lipid oxidation during storage and simulated gastrointestinal digestion, which was beneficial in fighting against the fight obesity. By the methyl thiazolyl tetrazolium assay, protein-proanthocyanidin nanoparticles exhibited no cytotoxicity for normal liver cells but significant cytotoxicity against liver hepatocellular carcinoma (HepG2 cells), thus have great potential in drug delivery (Liu, Li, Yang, Xiong, & Sun, 2017). There are now many studies on natural globulins, protein–polysaccharides, and protein-pectin-polyphenol complexes for the preparation of HIPPEs (Feng et al., 2021; Ribeiro, Morell, Nicoletti, Quiles, & Hernando, 2021; Xu, Tang, Liu, & Liu, 2018). However, the preparation of HIPPEs with protein–polyphenol composite particles needs more research.

In this study, we aim to prepare stable BSPI-C3G covalent composite particles and prepare Pickering emulsions with fish oil as the model-internal phase without surfactants. Therefore, we investigated the structure of BSPI-C3G particles by Fourier transform infrared spectroscopy (FTIR), X-ray diffraction (XRD), differential scanning calorimetry (DSC), and oil–water interfacial tension. In addition, the effects of BSPI-C3G particles with various BSPI concentrations and various ratios of oil phases for the preparation of Pickering emulsions were investigated by particle size, microstructure, Laser scanning confocal microscopy (LSCM), rheology, thermal stability, storage stability and oxidative stability (determination of hydrogen peroxide and secondary oxidation products). We expect this study to provide a new approach for the preparation of Pickering emulsions from BSPI-C3G particles and to be used to provide new bioactive ingredients in the food and pharmaceutical industries.

## 2. Materials and methods

### 2.1. Materials

BSPI (≥99 %) was purchased from Heilongjiang Heliang Agriculture Co., ltd. ( Harbin, China). Cyanidin-3-O-glucoside (C3G, purity ≥98 %) was purchased from Xi'an Ruilin Biotechnology Co., ltd. (Xi'an, China). Fish oil (contain 50 % DHA) was obtained from Xi'an Weisbo Biotechnology Co., ltd. (Xi'an, China). Nile red (≥95 %) was purchased from sigma (Shanghai, China). Fluorescein isothiocyanate (FITC, purity >95 %) was purchased from Shanghai Aladdin Biochemical Technology Co., ltd. (Shanghai, China). Cumene hydroperoxide (≥85 %) was purchased from Shanghai McLean Biochemical Technology Co., ltd. (Shanghai, China). 1,1,3,3- tetrathoxypropane (≥97 %) was purchased from Shanghai lianshuo Biotechnology Co., ltd. (Shanghai, China). All other chemicals used were of analytical grade and used as purchased.

### 2.2. Preparation of BSPI-C3G covalent complexes

BSPI-C3G covalent complexes were prepared by the previous research method (Ju et al., 2020). Briefly, 6.0 g of black soybean protein isolate (BSPI) was dispersed in 100 mL of ultrapure water to prepare the BSPI solution (6 %, w/v) with stirring for 2 h and separating from oxygen, then stored overnight at 4℃ to completely hydrate the protein. Then anthocyanin aqueous solution (0.15 %, w/v) was added and homogeneously mixed with freshly prepared BSPI solution (6 %, w/v) at a volume 1:1 ratio and the pH of the mixture was adjusted to 9.0 with stirring for 24 h in full contact with oxygen. Afterward, the pH was adjusted to 7.0, heated in a water bath at 95℃ for 15 min and cooled to room temperature to get the BSPI-C3G covalent complex (3 %, w/v). The various concentrations of BSPI-C3G covalent complex solutions were obtained by diluting the ultrapure water to BSPI-C3G concentrations (C) of 0.5 %, 1 %, and 2 % (w/v). The unreacted C3G was dialyzed in a 3500 kDa dialysis bag and the dialysates were replaced per 12 h, for 48 h in a 4℃ refrigerator. At the end of dialysis, the solution of BSPI-C3G was transferred to pre-freeze and dried by a freeze dryer, after which was ground into a powdered solid for reserve.

### 2.3. Fourier transform infrared (FTIR) spectroscopy

The infrared spectra of C3G, BSPI, and BSPI-C3G were obtained by FTIR device (BRUKER ALPHA, German). The sample powder was mixed with potassium bromide at a mass ratio of 1:100 and pressed it into 1–2 mm thin sheets by a tablet press. The infrared spectra were collected with 16 scans in the range of 4000–400 $cm^{-1}$ and resolution of 32 $cm^{-1}$.

### 2.4. X-ray diffraction (XRD) analysis

XRD patterns were determined on a Bruker D8 Advance diffractometer (Bruker company, Germany). The sample powder was laid flat on the glass plate, and the diffraction patterns were obtained with Cu Kα X-rays ($\lambda = 1.54060$ nm). The range of scan was from 5° to 70°, step size of 2θ and a scanning speed of 2°/min.

### 2.5. Differential scanning calorimetry (DSC)

The TAQ2000 calorimeter (American TA company, USA) was used to characterize thermal transformation curves of C3G, BSPI, and BSPI-C3G. About 10 mg of sample powder was sealed in a hermetic aluminum pan and heated from 30℃ to 200℃ at a rate of 10℃/min, and the transfer gas was 25 mL/min flow rate of nitrogen to obtain the DSC thermal map.

### 2.6. Determination of oil–water interfacial tension

The surface tension of 3600 s was monitored at room temperature for BSPI-C3G complex solutions of various BSPI-C3G concentrations (C, 0.5 %, 1 %, 2 % and 3 %, w/v). BSPI was used as a blank control group. The test started when the sample solutions and fish oil were left for 1 h. The droplet volume was set to 30 μL and a sample was collected per 30 s. The Young-Laplace equation is used to determine how oil–water interfacial tension varies with adsorption time.

### 2.7. Preparation of Pickering emulsion

Pickering emulsions were prepared with various oil-phase fractions (φ, 20 % ~ 78 %, v/v) and BSPI-C3G concentrations (C, 0.5 % ~ 3 %, w/v). The fish oil was added to the BSPI-C3G complex solutions and homogenized by FLUKO FM200A high shear dispersing mixer (FLUKO Equipment Shanghai Co., ltd., China) at 20,000 rpm for 3 min at 25℃.

### 2.8. Microscope

Microscopic changes in Pickering emulsion samples were observed by DFC 7000 T fluorescence microscope (Leica GmbH, Germany) with 400 × magnification at 25 °C. About 20 μL of Pickering emulsions were titrated into a glass slide and covered with a cover glass.

### 2.9. Droplet size distribution

The droplet size distributions of Pickering emulsions were analyzed by BT-9300ST laser particle size analyzer (Dandong bait Instrument Co., ltd. Liaoning, China) and expressed as volume-mean diameter ($D_{4,3}$). The particle absorption index of 0.001, the refractive index of 1.470 and the refractive index of dispersant of 1.330 were set.

### 2.10. Confocal laser scanning microscope (CLSM)

Add 10 μL of fluorescent dye solution (0.5 % FITC or 0.2 % Nile Red) to 1 mL of sample for dyeing. The microstructure was observed by the FluoView™ FV3000 Confocal Laser Scanning Microscope (OLYMPUS China, Beijing, China) with excitation wavelengths of 488 nm and 561 nm, respectively.

### 2.11. Rheological properties

The rheological properties of Pickering emulsions were investigated with Discovery Hybrid Rheometer HR-10 (TA, USA) with a parallel plate geometry (40 mm diameter), the fixed gap of 1 mm, strain 0.5 % and frequency scanning (0.1–10 Hz) at 25℃. All the samples were tested in the range of the linear viscoelastic zone.

### 2.12. Thermal stability of Pickering emulsion

The Pickering emulsions with various BSPI-C3G concentrations (C, 0.5 % ~ 3 %, w/v) and the oil-phase fraction (φ = 74 %, v/v) were heated in a water bath at 100℃ for 15 min, then microstructure, particle size distribution and rheological of emulsions were observed and measured.

### 2.13. Storage stability of Pickering emulsion

The Pickering emulsions with BSPI-C3G various concentrations (C, 0.5 % ~ 3 %, w/v) and the oil-phase fraction (φ = 74 %, v/v) were placed at 25℃ for 14 d. Then microstructure, particle size distribution and rheological of emulsions were observed and measured.

### 2.14. Oxidative stability of Pickering emulsion

The Pickering emulsions with various BSPI-C3G concentrations (C, 0.5 % ~ 3 %, w/v) at the oil-phase fraction (φ = 74 %, v/v) were placed at 50℃ for 14 d in the baking oven to accelerate the oxidation. The degree of emulsion corruption was determined by testing the content of primary hydroperoxide and secondary oxidation products per 2 d.

#### 2.14.1. Hydrogen peroxide measurement

The measurement of hydrogen peroxide referred to the method of Shi et al (2020). Briefly, 0.3 mL of the sample was mixed with 1.5 mL isooctane/isopropanol (3:1 v/v), following by vortexing continuously for 10 s and centrifugation at 2000 × g for 5 min to collect the upper solution. Then the upper solution (200 μL) was mixed with methanol/*n*-butanol mixture (2.8 mL, 2:1, v/v) and added $NH_4SCN$ (15 μL, 3.94 M) and $Fe^{2+}$ solution (15 μL, 0.132 M $BaCl_2$ and 0.144 M $FeSO_4$ mixed in the ratio of 1:1). The reaction's absorbance was measured at 510 nm using an ultraviolet spectrophotometer after 20 min. The lipid hydrogen peroxide was determined according to the cumene hydroperoxide standard curve.

#### 2.14.2. Measurement of secondary oxidation products

Secondary oxidation products were monitored by thiobarbituric acid reactive substances assay (TBARS) (Xiao, Li, & Huang, 2015). 1 mL emulsion was mixed with 2 mL thiobarbituric acid (TBA) reagent (15 % trichloroacetic acid and 0.375 % TBA in 0.25 M HCl). Boiling the mixture in a water bath for 15 min, the mixture was cooled immediately to room temperature and used 1.2 μm microporous membrane filter. The absorbance of the mixture was measured by ultraviolet spectrophotometer at 532 nm. The secondary oxidation products were determined according to the 1,1,3,3-tetrathoxypropane standard curve.

### 2.15. Statistical analysis

One-way analysis of variance (ANOVA) was performed to compare the differences and differences were considered statistically significant when $p < 0.05$ using the SPSS 18.0 (SPSS Inc., Evanston, IL, USA). All experiments were formed with at least three replications. Results were expressed as mean ± standard deviation (SD).

## 3. Results and discussion

### 3.1. Interaction of BSPI-C3G particles and analysis of oil–water interfacial tension

FTIR spectroscopy can be used to characterize the interaction between BSPI and C3G through changes of characteristic absorption band shifts and intensities. Fig. 1A shows that the characteristic peaks of BSPI appeared in the amide A band (3100–3500 $cm^{-1}$), amide I band (1750–1600 $cm^{-1}$) and amide II band (1550–1510 $cm^{-1}$), which represented the stretching of N—H bond and the change of hydrogen bond, the stretching of C═O bond, the bending of C—N bond, and N—H bond, respectively (Dai, Sun, Wei, Mao, & Gao, 2018). The absorption bands of C3G at 1338 $cm^{-1}$, 1502 $cm^{-1}$, and 1634 $cm^{-1}$ were mainly, which were due to C═C stretching of the aromatic ring, the stretching and bending vibration of the alkane C—H bond, and = C—H bending of the aromatic ring. While at 3407 $cm^{-1}$, it was produced mainly by vibrational stretching of phenolic hydroxyl group (Chen et al., 2020). The BSPI-C3G covalent complexes had a wider characteristic peak at 3286 $cm^{-1}$ compared to the characteristic peak of C3G. The results indicated that the number of hydroxyl groups increased with higher covalent binding of BSPI to C3G, due to the stretching vibration of C-OH, which was consistent with the results of Qin et al (2021). Compared with the characteristic peaks of BSPI, the absorption peak at 3428 $cm^{-1}$ corresponding to the hydrogen bond in the BSPI-C3G particles redshifted to 3286 $cm^{-1}$ in the covalent composite particles. The absorption vibration of the amide A band may come from the hydrogen bond or the stretching vibration of the O—H bond. The shift of absorption wave number from large wave number to small wave number indicated that a new hydrogen bond has been formed between BSPI and C3G. By studying the infrared spectra of zein and epigallocatechin (EGCG), He et al (2020) found that the absorption peak at 3412 $cm^{-1}$ corresponding to the hydrogen bond in zein redshifted to 3406 $cm^{-1}$ in the composite nanoparticles, indicating that a new hydrogen bond between the hydroxyl group of EGCG and the amide group of zein was formed.

As shown in Fig. 1B, the diffraction spectrum of C3G showed a multi-peak shape, indicating a highly crystalline structure with a directional and orderly arrangement (He et al., 2020). The 10° and 20° diffraction peaks of protein were shown in the XRD study α-Spiral and β-Folding structure (Chen, Chen, Zhu, Chen, Zhao, & Ao, 2013). BSPI had obvious diffraction peaks at about 9° and 20°, and the intensity of the diffraction peak at 20° was much greater than 9°. The results indicated that the β-Folding of the secondary structure in the BSPI was dominant and was important for protein stability. After the addition of C3G, there was no new diffraction peak but the diffraction intensity at 10° and 20° decreased in BSPI-C3G, indicating that no new crystal structure was generated between them in the covalent complex and the protein structure changed from crystal to amorphous structure. A similar result was also observed in another study of soy peptide-based nanoparticle (SPN) loaded curcumin (Zhang, Zhao, Ning, Yu, Tang, & Zhou, 2018). Additionally, the characteristic crystal diffraction peak of anthocyanin almost completely disappeared, suggesting that anthocyanin was embedded in the complex matrix of BSPI in an amorphous state (Li et al.,

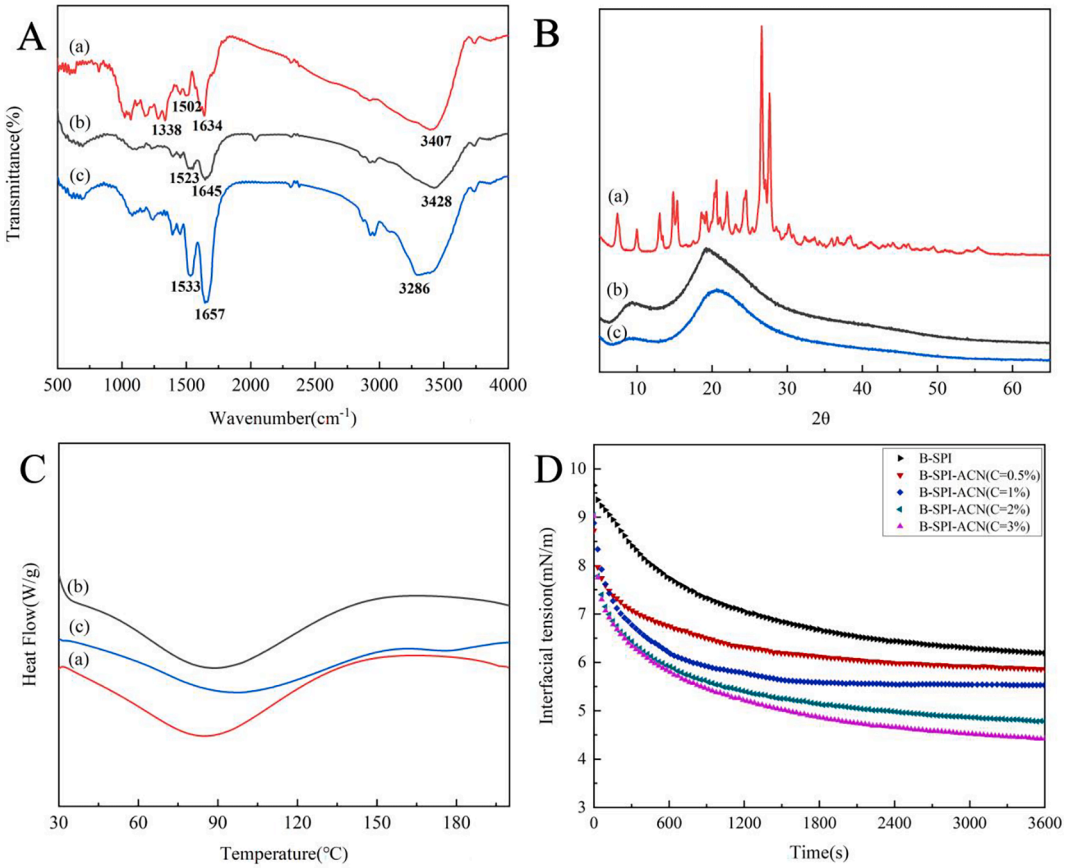


**Fig. 1.** FTIR spectra (A), XRD spectrums (B) and DSC thermograms (C) of C3G (a), BSPI (b) and BSPI-C3G covalent complex (c). the oil–water interfacial tension diagram (D) of particles with various BSPI-C3G concentrations (C, 0.5 %, 1 %, 2 %, and 3 %, w/v), and the blank control group was BSPI without C3G.

2019). As expected, the results of XRD match FTIR.

DSC technique is one of the advanced methods to study the compatibility of polymers by controlling the temperature. Peak temperature ($T_P$) can indicate protein denaturation and higher $T_P$ was closely associated with higher thermal stability and tighter tertiary conformation proteins (Diedericks, Shek, Jideani, Venema, & Linden, 2020; Tang, Sun, & Foegeding, 2011). Fig. 1C shows that there was an endothermic melting peak for C3G at 97.13℃, but no peak shape for the complex, suggesting that the crystal morphology of the anthocyanins has changed. After interacting with C3G, the $T_P$ of BSPI decreased from 88.97℃ to 84.40℃, which also observed similar phenomena in other C3G-protein systems (Ren, Xiong, Li, & Li, 2019). Therefore, C3G could change the stability of the tertiary structure of BSPI, which was conducive to improve the emulsifying performance of protein and produce smaller lipid droplets (Tang et al., 2011).

Generally, the stability of Pickering emulsions is dependent on their interfacial strength. Some small molecule surfactants typically have a lower interfacial strength, which could further cause destruction of the emulsion. Fig. 1D shows the trend of oil–water interfacial tension of the BSPI-C3G complexes with time. The interfacial tension of sample solutions decreased rapidly, and protein was adsorbed on the oil–water interface within 1200 s. The interfacial decreased slowly, and a relatively stable protein adsorption membrane was gradually formed at the oil–water interface after 1200 s (Hu et al., 2016). Moreover, the BSPI-C3G complexes were found to be more readily absorbed at the oil–-water interface than BSPI. Kim & Shin (2016) obtained similar results by studying the interfacial tension of bovine serum albumin fucoidin conjugate prepared by Maillard reaction. In Addition, the potential effect of concentration on the adsorption of BSPI-C3G covalent complexes at the oil–water interface was also discussed, and it was found that the interfacial tension decreased as the concentrations of the covalent complexes increased. This was similar to the structure of previous studies, and the concentrations of the complex were found to affect the interfacial arrangement and interfacial layer thickness, with higher concentrations of particles increasing the interfacial layer thickness and further increasing the stability of the emulsion (Qin et al., 2021).

### 3.2. *Characteristics and particle size distribution of Pickering emulsion*

The Pickering emulsion with BSPI-C3G complexes could be fast dispersed in distilled water but keep granular aggregate in the oil, thus it was an O/W type (Qin et al., 2021). Fig. 2A shows the stability of the Pickering emulsions with various BSPI-C3G concentrations (C, 0.5 %–3 %, w/v) and oil phase fractions (φ, 20 %–78 %, v/v). The Pickering emulsions with various BSPI-C3G concentrations formed layers rapidly at the oil phase fraction (φ) lower than 60 % (v/v) (Kaganyuk & Mohraz, 2019). With the oil phase fraction (φ) increased, the emulsion layer of the Pickering emulsion increased significantly and the inverted emulsion did not flow downward, possibly forming a homogeneous gel emulsion. To further determine whether the Pickering emulsion was a concentrated emulsion or a hydrogel, a part of the Pickering emulsion (about 0.15–0.2 g) was mixed with distilled water or 6 M urea in the weight ratio of 1:10 and then incubated at 25 °C for 12 h. The morphology and microstructure of the prepared dispersions were evaluated by visual observation and optical microscope after vortexing for 10 s. In Fig. 2B, the dispersion behavior of the emulsion in distilled water or 6 M urea was similar, and urea did not cause any damage to the droplet structure, indicating that the emulsion formed a gel-like structure when the oil phase fraction was greater than 70 % (v/v) (Xu, Liu, & Tang, 2018).

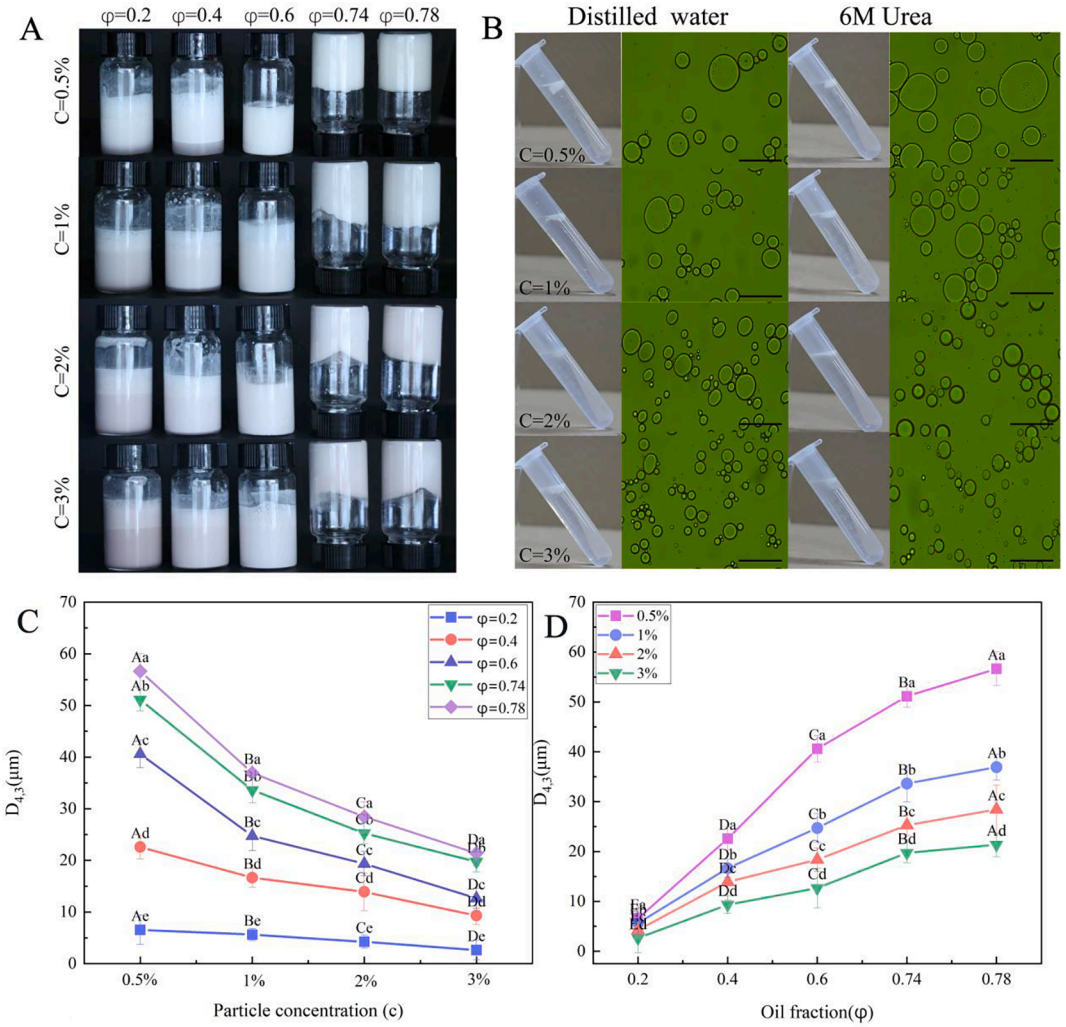


**Fig. 2.** A: The visual observation of Pickering emulsions with various BSPI-C3G concentrations (C, 0.5 %, 1 %, 2 % and 3 %, w/v) and oil-phase fractions (φ, 20 %, 40 %, 60 %, 74 % and 78 %, v/v). B: Visual observation and optical microscope of Pickering emulsions with various BSPI-C3G concentrations (C) and fixed oil phase fraction (φ, 74 % v/v) in distilled water and 6 M urea. C: Particle size ($D_{4,3}$) analysis of Pickering emulsions with various oil-phase fractions (φ) and fixed BSPI-C3G concentration (C, 1 %, w/v). D: $D_{4,3}$ analysis of Pickering emulsions with various BSPI-C3G concentrations (C) and fixed oil-phase fraction (φ, 74 %, v/v).

Fig. 2C and Fig. 2D show the $D_{4,3}$ of Pickering emulsions with various BSPI-C3G concentrations (C, 0.5 % ~ 3 %, w/v) and oil phase fractions (φ, 20 % ~ 78 %, v/v). The $D_{4,3}$ of the Pickering emulsion increased with an increase in the oil phase fractions when the particle concentration was constant. When the particle concentration was fixed 0.5 % (w/v) and the oil phase fractions increased from 20 % to 78 % (v/v), the $D_{4,3}$ reached from 6.55 ± 2.85 μm to 56.64 ± 3.3 μm. There was a possibility that the low concentration complex particles cannot completely enclose the fish oil, and the $D_{4,3}$ became larger as droplets undergo aggregation (Li et al., 2020). When the oil phase fraction was 74 % (v/v) and the BSPI-C3G concentrations increased from 0.5 % to 3 % (w/v), the $D_{4,3}$ of the Pickering emulsions decreased with increasing oil phase fractions, and the droplet size decreased from 51.12 ± 2.16 μm to 19.72 ± 1.95 μm. The higher concentration of BSPI-C3G could stabilize more oil droplets, probably because the higher concentration of composite particles had a larger interfacial layer thickness, which wrapped around smaller oil droplet and reduced the $D_{4,3}$ of the Pickering emulsions (Sun, Zhong, Zhao, Li, Qi, & Jiang, 2022). It had been found that large size droplets could be formed by hydrophobic interaction, at low particle concentrations and oil phase fractions, while small size droplets were squeezed into bridging monolayers at high BSPI-C3G concentrations and oil phase fractions (Ju et al., 2020).

### 3.3. Confocal microstructure of Pickering emulsion

Fig. 3 shows that HIPPEs (φ = 74 %, v/v) prepared with various BSPI-C3G concentrations were characterized by CLSM. The fluorescent structures of oil and water were superimposed, the fish oil was stained red by Nile Red, and the BSPI-C3G complex particles were stained green by FITC. It can be clearly observed that the red oil droplets were separated into individual grids by the green BSPI-C3G solution, indicating that the BSPI-C3G complex particles formed a stable structure on the surface of the oil droplets, and the oil droplets formed a crowded but non-aggregated state as the filler of the network structure, forming a typical O/W Pickering emulsion (Feng et al., 2021). When the HIPPEs with the BSPI-C3G particles concentration (C = 0.5 %, w/v), the droplets were not uniformly distributed and most of them had independent interfaces with a particle size of about 50 μm, which was consistent with the results of $D_{4,3}$. When the concentration of BSPI was increased to 3 % (w/v), the distribution of droplets was more uniform and the particle size of the droplets became significantly smaller. The reason for this result may be because the particle concentration increased and the combination of C3G-BSPI improved the hydrophilicity of the protein and better inhibited the aggregation between droplets (Ju et al., 2020; Liu, Guo, Wan, Liu, Ruan, & Yang, 2018).

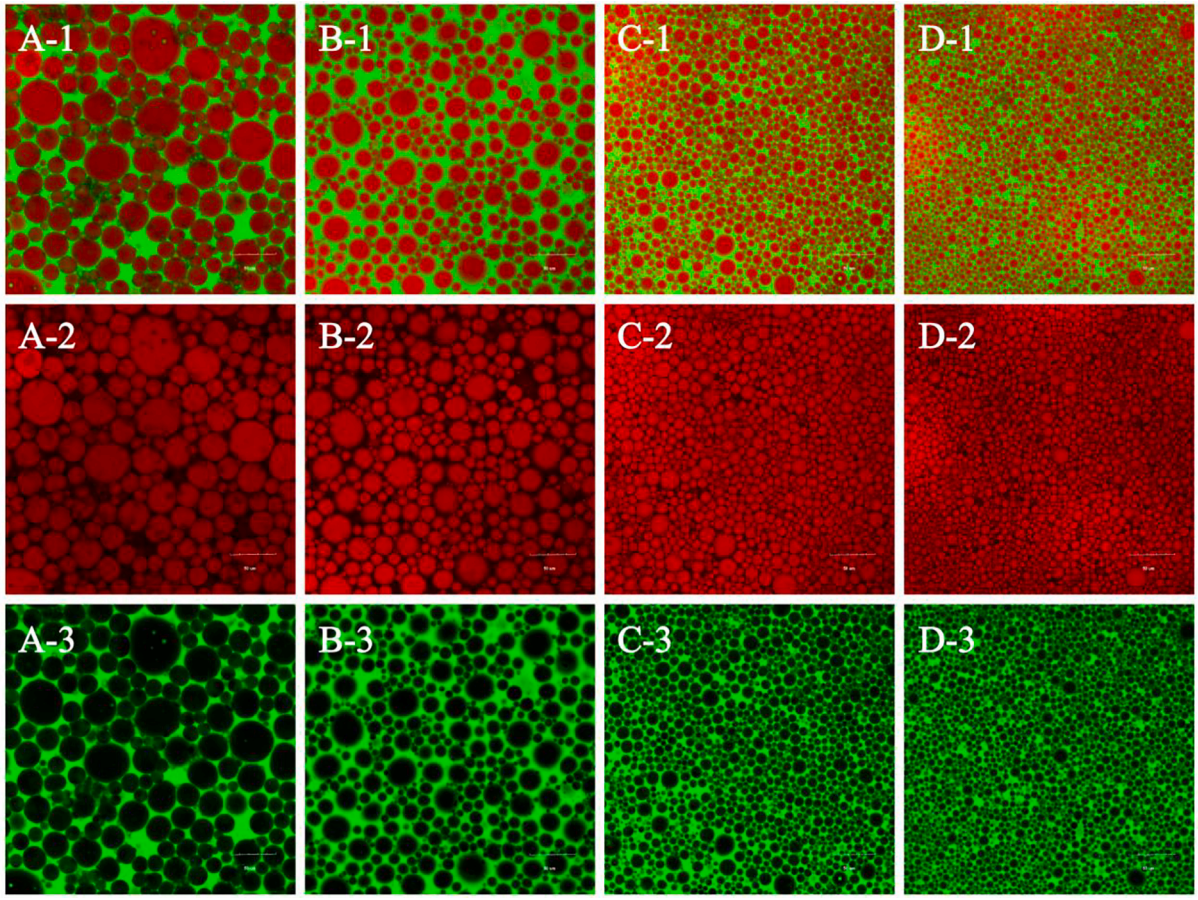


**Fig. 3.** The CLSM images with various BSPI-C3G concentrations (C, 0.5 %, 1 %, 2 % and 3 %, w/v) and fixed oil-phase fraction (φ, 74 %, v/v). (A1-D1): overlapping fluorescence images of oil and water; (A2-D2): oil phase fluorescence images; (A3-D3): BSPI-C3G solution fluorescence images.

### *3.4. Visual and microscopic observation and rheological properties of Pickering emulsion*

Fig. 4A shows the sizes of the Pickering emulsions at the various BSPI-C3G concentrations and oil phase fractions were about 10–50 μm. When oil phase fractions were 20 %, 40 %, and 60 % (v/v), the droplets showed small size spheres dispersed in the emulsions. The droplets of the Pickering emulsions formed at the oil phase (φ, 74 % and 78 %, v/v) were small and polygonal, and the increase in repulsion force between BSPI-C3G complex particles was considered an important contribution (Ju et al., 2020).

An important indicator to evaluate the stability of Pickering emulsions is the rheological properties, of which the storage modulus (G') and loss modulus (G'') might reflect the macroscopic viscoelastic properties of the interfacial films (Liu, Liu, Wang, & Li, 2021). The rheological properties of Pickering emulsions prepared with various BSPI-C3G concentrations and oil phase fractions are shown in Fig. 4B and Fig. 4C. For all of the samples, G' was always larger than G'', showing frequency dependence, which indicated that the Pickering emulsion might form a high internal phase gel structure. The interconnected network formed between the adsorbed and without adsorbed protein particles in the emulsions also improved the elasticity of the emulsion (Xu et al., 2021). With the increase of BSPI-C3G particle concentration, the elasticity of emulsion gradually increased and then remained at a relatively high level, which may be due to the increase in the number of droplet–droplet interactions, indicating that BSPI-C3G particle-stabilized Pickering emulsion with an interfacial three-dimensional network promoted the formation of the elastic gel-emulsion network (Liu et al., 2020). In contrast, when the particle concentration was constant, the viscoelasticity of the Pickering emulsion increased as the volume of the oil phase increased. When the oil phase fraction was 78 % (v/v), it was indicated that the emulsion had the best viscoelasticity and the strongest gel was formed. In addition, the increasing oil phase fraction also had a significant effect on the viscoelasticity of the emulsion droplets.

### *3.5. Thermal stability analysis*

Heating is a common operation unit in food processing. Fig. 5 shows the visual and microstructure observations, particle size distribution and rheological properties of HIPPEs with oil phase fraction ($\varphi = 0.74$, v/v) and various BSPI-C3G concentrations (C = 0.5 % ~ 3 % w/v) upon heating (at 100°C for 15 min). After heating, the particle size of HIPPEs (Fig. 5A and B) stabilized with BSPI-C3G concentrations (C = 0.5 % and 1 %, w/v) increased significantly from 52.57 ± 2.0 and 31.66 ± 2.9 μm to 104.6 ± 3.9 and 53.57 ± 1.3 μm, respectively ($P < 0.05$). Droplet size of HIPPEs stabilized with BSPI-C3G concentration (C = 3 %, w/v) did not significantly ($p > 0.05$). Obviously, the droplet stability of the emulsions was enhanced with increasing BSPI-C3G particle concentrations. This may be because the oil droplets' surface was tightly adsorbed by the BSPI-C3G particles, and the energy provided by heating was not enough to separate the oil from the protein particles, thus the high concentration of BSPI-C3G could better maintain the thermal stability of the emulsion (Zhu, Zhang, Huang, & Xiao, 2021). As shown in Fig. 5C, the elasticity of HIPPE after heating increased with increasing concentration of BSPI-C3G concentration but the increase was not significant when the BSPI-C3G concentration was higher ($p < 0.05$). The reason was supposed to be that the protein structure of the low protein

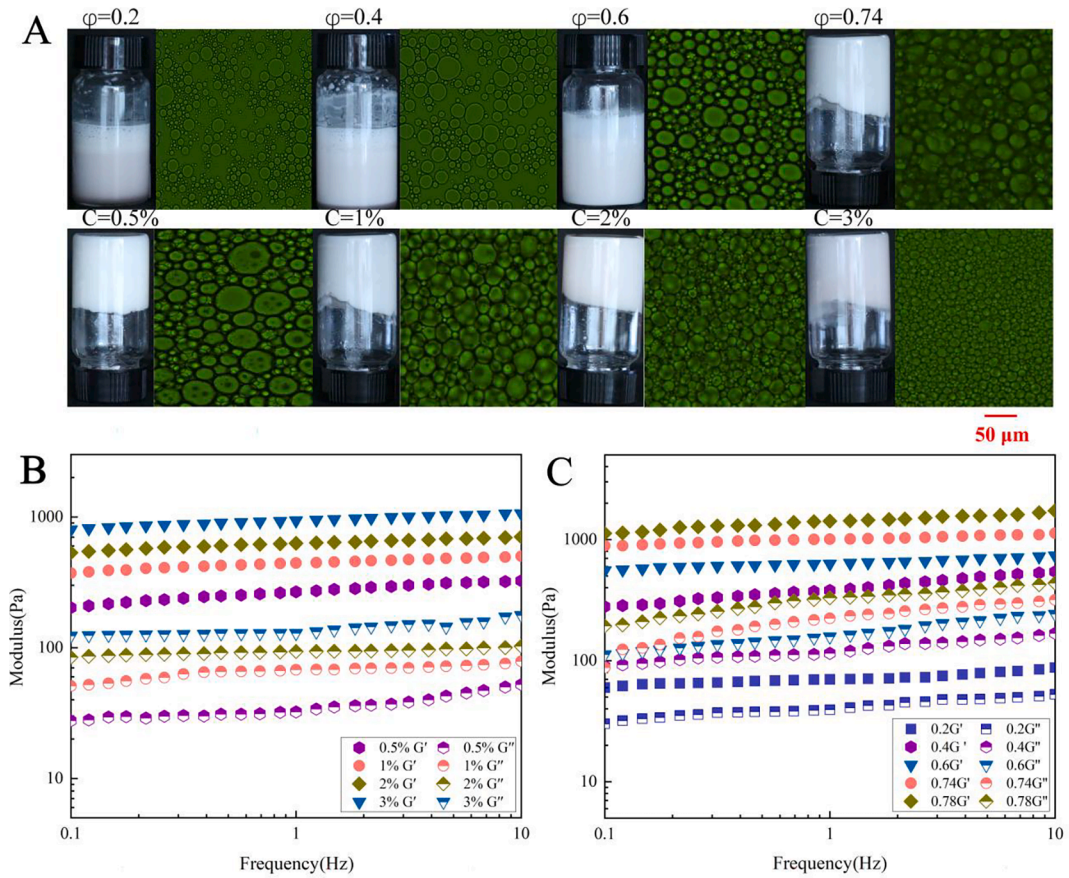


**Fig. 4.** A: The visual observation and optical microscope of Pickering emulsions with fixed BSPI-C3G concentration (C, 1 %, w/v) and various oil-phase fractions (φ, 20 %, 40 %, 60 % and 74 %, v/v), and fixed oil-phase fraction (φ, 74 %, v/v) and various BSPI-C3G concentrations (C, 0.5 %, 1 %, 2 % and 3 %, w/v). B: Rheological properties of HIPPEs with fixed oil-phase fraction (φ, 74 %, v/v) and various BSPI-C3G concentrations (C, 0.5 %, 1 %, 2 % and 3 %, w/v). C: Rheological properties of Pickering emulsions with fixed BSPI-C3G concentration (C, 1 %, w/v) and various oil-phase fractions (φ, 20 %, 40 %, 60 %, 74 % and 78 %, v/v).

concentration was rearranged during the heating process. Furthermore, the heating-induced protein denaturation enhanced the interaction between adsorbed and without adsorbed protein particles when the protein concentration became higher. This effect may compensate for the effect of structural rearrangement on elasticity thus the elasticity of Pickering emulsion was significantly improved during heating (Xu, Liu, et al., 2018).

### 3.6. Storage stability analysis

The visual and microstructure observations, particle size distribution and rheological of HIPPEs with oil phase fraction (φ = 0.74, v/v) and various BSPI-C3G concentrations (C = 0.5 % ~ 3 % w/v) were stored at 25℃ for 14 d (Fig. 6A-C). The $D_{4,3}$ of HIPPEs stabilized with BSPI-C3G (0.5 % w/v) increased significantly after 14 d of storage at room temperature (Fig. 10A). However, the particle size of the emulsions gradually stabilized as the BSPI-C3G concentration increased. When the BSPI-C3G concentration was 3 % (w/v), the $D_{4,3}$ of the emulsions changed from 14.53 ± 1.6 μm to 15.26 ± 0.83 μm, with almost no significant difference ($P < 0.05$). This may be due to the high concentration of molecular polymers preventing the droplets from moving with each other and improving the stability of the emulsion (Zhang et al., 2018). Fig. 6B shows more clearly that the D4,3 of HIPPEs emulsions gradually decreases with increasing BSPI-C3G concentration but the D4,3 variation becomes less and less significant. The particle size of Pickering emulsion becomes smaller, which is consistent with the microstructure. Therefore, the Pickering emulsion with high particle stability was more stable. When the BSPI-C3G concentration was 0.5 % (w/v), the $D_{4,3}$ of the Pickering emulsion increased from 46.26 ± 1.2 μm to 63.7 ± 3.0 μm. Although the particle size of the Pickering emulsion increased obviously, it still possessed some characteristics of a high internal phase Pickering emulsion. This may be attributed to the addition of anthocyanins promoting the hydrophobic interaction between C3G and BSPI, and improving the interfacial wettability of the complexes, and resulting in certain stability of the Pickering emulsion (Feng et al., 2021). By observing the rheological properties of different emulsions before and after storage, it was found that the G′ of the emulsions did not change much when the BSPI-C3G concentrations were 2 % and 3 % (v/v), which indicated that the BSPI-C3G complex could stabilize the HIPPEs very well (Liu et al., 2018).

### 3.7. Oxidation stability analysis

The oxidative stability of the Pickering emulsion was determined by measuring the content of lipid hydrogen peroxide (LH) and malondialdehyde (MDA) (Fig. 6D and Fig. 6E). BSPI-C3G particles significantly stabilized Pickering emulsions and reduced the content of LH and MDA. As shown in Fig. 6D, the hydroperoxides of all samples showed an upward trend during storage, indicating that the fish oil had an oxidation reaction. At the same time, compared with the fish oil in the blank control group, the lipid oxidation value gradually decreased with the increase of the concentrations of BSPI-C3G from 15.1 mmol/L to 7.9 mmol/L. For oil in water emulsion, the composition and structure of the oil–water interface played a key role in regulating the rate and degree of lipid oxidation. Meanwhile, the changing trend of MDA was basically the same as that of hydroperoxide. With the increase in BSPI-C3G

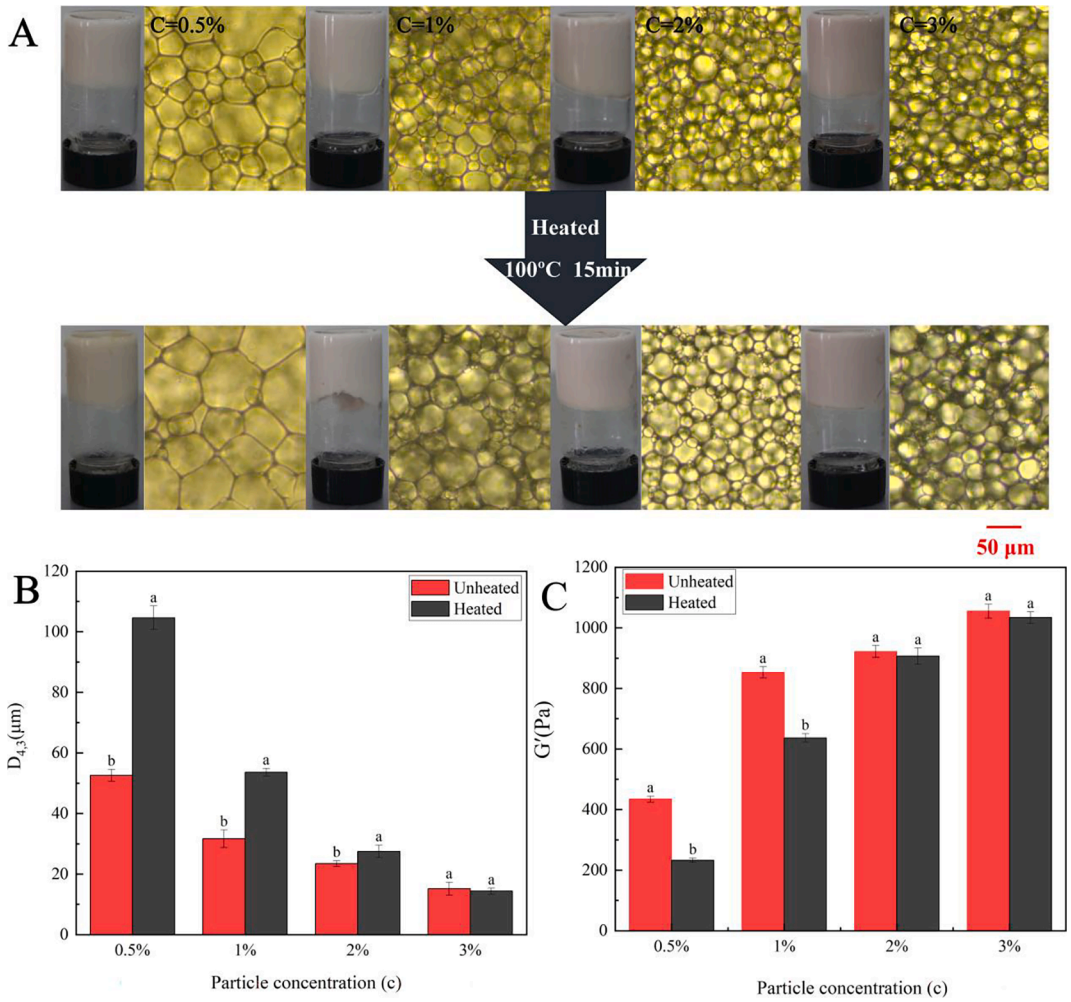


**Fig. 5.** The appearance and microstructure (A), $D_{4,3}$ (B), and rheological properties (C) of HIPPEs with various BSPI-C3G concentrations (C, 0.5 %, 1 %, 2 %, and 3 %, w/v) were heated in a water bath at 100℃ for 15 min. Values with different superscript letters are significantly different ($p < 0.05$).

concentrations, the MDA content decreased from 4.5 mmol/L to 1.2 mmol/L. Zou et al (2017) reported that zein-tannic acid stabilized Pickering emulsion also inhibited the formation of MDA in the oxidation process. In this study, the content of LH and MDA gradually decreased, indicating that the BSPI-C3G particles stabilized Pickering emulsion had good oxidation stability. The complex particles further blocked the lipid hydrogen peroxide and scavenged free radical chain reaction by blocking the interaction between LH and oxidant and played the role of lipid oxidation barrier. In addition, because the antioxidant sites of anthocyanins were on phenolic hydroxyl groups, phenolic hydroxyl groups reacted with free radicals produced by lipid oxidation to inhibit the oxidation of oils and fats. The study also showed that the structure of Pickering emulsion may help inhibit the transfer from the aqueous phase to the interfacial region (Zhou et al., 2018).

## 4. Conclusion

In conclusion, as a novel food-grade particle stabilizer, BSPI-C3G covalent particles with a high amount of C3G grafting fabricated under alkalescence conditions could be applied for the preparation of HIPPEs successfully. Stable HIPPEs can be formed with low particle concentrations (C, 0.5 %–3 %, w/v). The microstructure of HIPPEs was observed by CLSM which confirmed the BSPI-C3G particles formed a dense particle layer around the surfaces of the oil droplets. In addition, the oil droplets formed a crowded but non-aggregated state as the filler of the network structure. The storage modulus (G') was higher than loss modulus (G''), showing a clear frequency dependence. The appearance and the rheological characteristics of HIPPEs verified the gel-like state. Particle concentration was an important factor to affect the stability of HIPPEs by modifying the structural and physical properties of them. As the concentration of BSPI-C3G increased, the emulsion droplet size gradually decreased and the emulsion droplet distribution was more uniform. Pickering emulsions with different concentrations of BSPI-C3G inhibited the oxidation of oil to some extent but the HIPPEs with excellent stability could be obtained at the 3 % (w/v) BSPI-C3G particle concentration. This study prepared new solid particles with BSPI and C3G and successfully prepared Pickering emulsions, which provided a reference for the research of new stabilizers and also increased the added value of BSPI and C3G. Then the gel-like HIPEs were stabilized entirely by food-grade ingredients which might have a wide range of applications in food.

## CRediT authorship contribution statement

**Xiaojie Cui:** Methodology, Validation, Formal analysis, Investigation, Visualization, Writing – original draft. **Mengyao Ma:** Methodology, Conceptualization, Formal analysis, Investigation, Software, Writing – original draft. **Yanli Xie:** Methodology, Conceptualization, Supervision, Funding acquisition, Writing – review & editing. **Yuhui Yang:** Methodology, Project administration, Visualization, Conceptualization, Writing – review & editing. **Qian Li:** Methodology, Project administration, Visualization. **Shumin Sun:** Methodology, Project

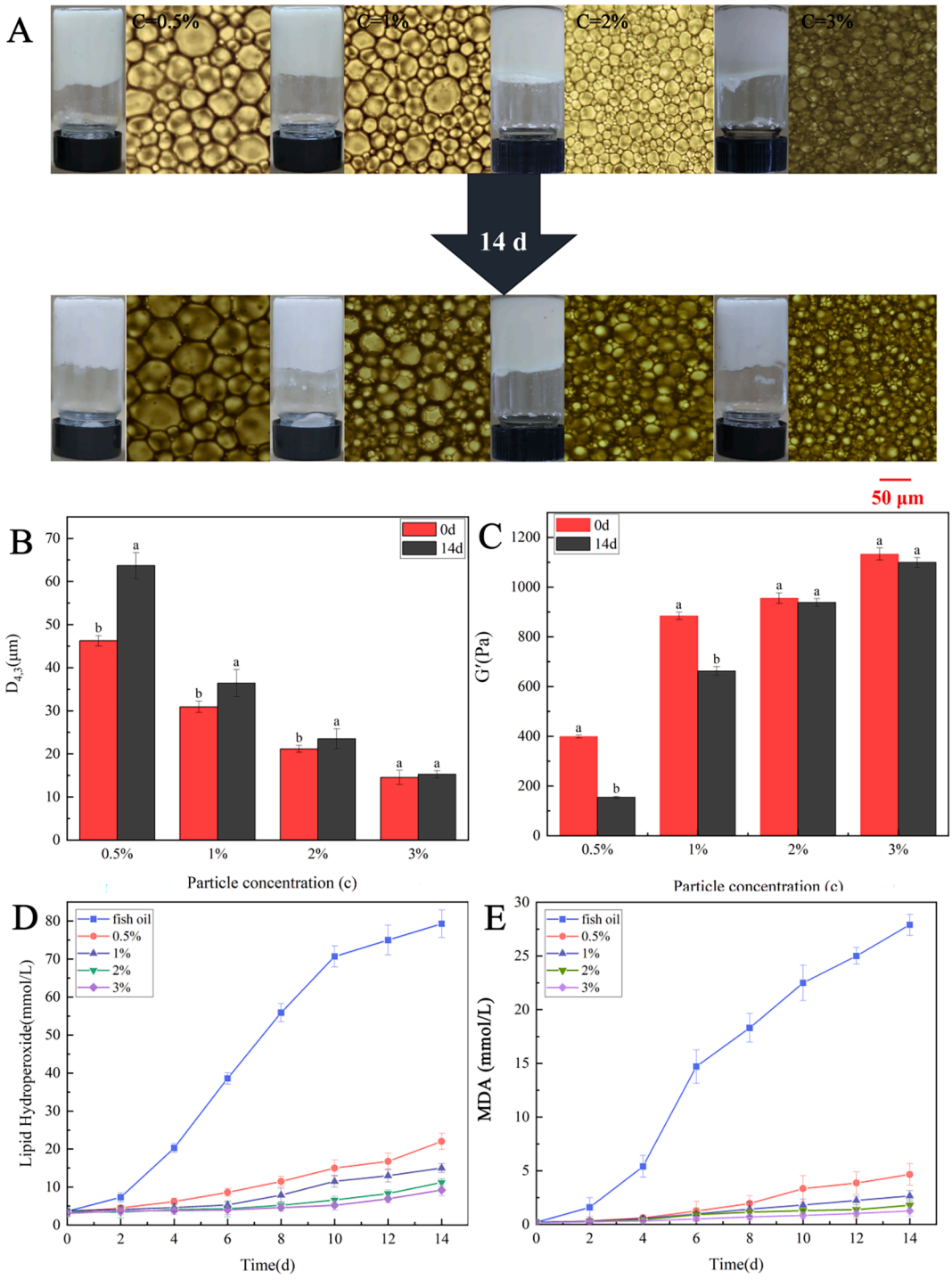


**Fig. 6.** The appearance and microstructure (A), $D_{4,3}$ (B) and rheological properties (C) of HIPPEs with various BSPI-C3G concentrations (C, 0.5 %, 1 %, 2 % and 3 %, w/v) were stored at 25℃ for 14 d; Lipid hydroperoxides (D) and malondialdehyde (E) of lipid oxidation products of HIPPEs with various BSPI-C3G concentrations (C, 0.5 %, 1 %, 2 % and 3 %, w/v) at 50℃. Values with different superscript letters are significantly different ($p < 0.05$).

administration, Visualization. **Weibin Ma:** Methodology, Project administration, Visualization.

## Declaration of Competing Interest

The authors declare that they have no known competing financial interests or personal relationships that could have appeared to influence the work reported in this paper.

## Acknowledgements

This work was supported by the National Natural Science Foundation of China (No. 31972003) and the Program for Innovative Research Team (in Science & Technology) at the University of Henan Province (No. 20IRTSTHN023).

## Reference


Chen, J., Chen, X., Zhu, Q., Chen, F., Zhao, X., & Ao, Q. (2013). Determination of the domain structure of the 7S and 11S globulins from soy proteins by XRD and FTIR. *Journal of the Science of Food & Agriculture, 93*(7), 1687–1691. https://doi.org/10.1002/jsfa.5950

Chen, S., Shen, X., Tao, W., Mao, G., Wu, W., Zhou, S., … Pan, H. (2020). Preparation of a novel emulsifier by self-assembling of proanthocyanidins from Chinese bayberry (Myrica rubra Sieb. et Zucc.) leaves with gelatin. *Food Chemistry, 319*, Article 126570. https://doi.org/10.1016/j.foodchem.2020.126570

Chen, Z., Wang, C., Gao, X., Chen, Y., Santhanam, R., Wang, C., … Chen, H. (2019). Interaction characterization of preheated soy protein isolate with cyanidin-3-O-glucoside and their effects on the stability of black soybean seed coat anthocyanins extracts. *Food Chemistry, 271*, 266–273. https://doi.org/10.1016/j.foodchem.2018.07.170

Diedericks, C. F., Shek, C., Jideani, V. A., Venema, P., & Linden, E. (2020). Physicochemical properties and gelling behaviour of Bambara groundnut protein isolates and protein-enriched fractions. *Food Research International, 138*, Article 109773. https://doi.org/10.1016/j.foodres.2020.109773

Feng, T., Wang, X., Wang, X., Zhang, X., Gu, Y., Xia, S., & Huang, Q. (2021). High internal phase pickering emulsions stabilized by pea protein isolate-high methoxyl pectin-EGCG complex: Interfacial properties and microstructure. *Food Chemistry, 350*, Article 129251. https://doi.org/10.1016/j.foodchem.2021.129251

Fu, X., Belwal, T., He, Y., Xu, Y., Li, L., & Luo, Z. (2020). Interaction and binding mechanism of cyanidin-3-O-glucoside to ovalbumin in varying pH conditions: A spectroscopic and molecular docking study. *Food Chemistry, 320*, Article 126616. https://doi.org/10.1016/j.foodchem.2020.126616

Fu, X., Wang, D., Belwal, T., Xu, Y., Li, L., & Luo, Z. (2021). Sonication-synergistic natural deep eutectic solvent as a green and efficient approach for extraction of phenolic compounds from peels of Carya cathayensis Sarg. *Food Chemistry, 355*, Article 129577. https://doi.org/10.1016/j.foodchem.2021.129577

He, A., Guan, X., Song, H., Li, S., & Huang, K. (2020). Encapsulation of (-)-epigallocatechin-gallate (EGCG) in hordein nanoparticles. *Food Bioscience, 37*, Article 100727. https://doi.org/10.1016/j.fbio.2020.100727

Hu, Y., Yin, S., Zhu, J., Qi, J., Guo, J., Wu, L., … Yang, X. (2016). Fabrication and characterization of novel Pickering emulsions and Pickering high internal emulsions stabilized by gliadin colloidal particles. *Food Hydrocolloids, 61*, 300–310. https://doi.org/10.1016/j.foodhyd.2016.05.028

Ju, M., Zhu, G., Huang, G., Shen, X., Zhang, Y., Jiang, L., & Sui, X. (2020). A novel pickering emulsion produced using soy protein-anthocyanin complex nanoparticles. *Food Hydrocolloids, 99*, Article 105329. https://doi.org/10.1016/j.foodhyd.2019.105329

Kaganyuk, M., & Mohraz, A. (2019). Role of particles in the rheology of solid-stabilized high internal phase emulsions. *Journal of Colloid and Interface Science, 540*, 197–206. https://doi.org/10.1016/j.jcis.2018.12.098

Kim, D.-Y., & Shin, W.-S. (2016). Functional improvements in bovine serum albumin-fucoidan conjugate through the Maillard reaction. *Food Chemistry, 190*, 974–981. https://doi.org/10.1016/j.foodchem.2015.06.046

Li, H., Wang, D., Liu, C., Zhu, J., Fan, M., Sun, X., … Cao, Y. (2019). Fabrication of stable zein nanoparticles coated with soluble soybean polysaccharide for encapsulation of quercetin. *Food Hydrocolloids, 87*, 342–351. https://doi.org/10.1016/j.foodhyd.2018.08.002

Li, J., Wang, B., He, Y., Wen, L., Nan, H., Zheng, F., … Zhang, H. (2021). A review of the interaction between anthocyanins and proteins. *Food Science and Technology International, 27*(5), 470–482. https://doi.org/10.1177/1082013220962613

Li, S., Sun, J., Yan, J., Zhang, S., Shi, C., McClements, D. J., … Liu, F. (2020). Development of antibacterial nanoemulsions incorporating thyme oil: Layer-by-layer self-assembly of whey protein isolate and chitosan hydrochloride. *Food Chemistry, 339*, Article 128016. https://doi.org/10.1016/j.foodchem.2020.128016

Liu, B., Liu, B., Wang, R., & Li, Y. (2021). α-Lactalbumin self-assembled nanoparticles with various morphologies, stiffnesses, and sizes as pickering stabilizers for oil-in-water emulsions and delivery of curcumin. *Journal of Agricultural and Food Chemistry, 69*(8), 2485–2492. https://doi.org/10.1021/acs.jafc.0c06263

Liu, C., Li, M., Yang, J., Xiong, L., & Sun, Q. (2017). Fabrication and characterization of biocompatible hybrid nanoparticles from spontaneous co-assembly of casein/gliadin and proanthocyanidin. *Food Hydrocolloids, 73*, 74–89. https://doi.org/10.1016/j.foodhyd.2017.06.036

Liu, X., Guo, J., Wan, Z., Liu, Y., Ruan, Q., & Yang, X. (2018). Wheat gluten-stabilized high internal phase emulsions as mayonnaise replacers. *Food Hydrocolloids, 77*, 168–175. https://doi.org/10.1016/j.foodhyd.2017.09.032

Liu, Y., Yan, C., Chen, J., Wang, Y., Liang, R., Zou, L., … Liu, W. (2020). Enhancement of beta-carotene stability by encapsulation in high internal phase emulsions stabilized by modified starch and tannic acid. *Food Hydrocolloids, 109*, Article 106083. https://doi.org/10.1016/j.foodhyd.2020.106083

Ma, M., Xie, Y., & Wang, C. (2021). Effect of anthocyanin-rich extract from black soybean coat on wheat dough rheology and noodle texture. *Journal of Food Processing and Preservation, 45*(1), 15007. https://doi.org/10.1111/jfpp.15007

Ma, Z., Cheng, J., Jiao, S., & Jing, P. (2022). Interaction of mulberry anthocyanins with soybean protein isolate: Effect on the stability of anthocyanins and protein in vitro digestion characteristics. *International Journal of Food Science and Technology, 57*(4), 2267–2276. https://doi.org/10.1111/ijfs.15576

Qin, X., Gao, Q., & Luo, Z. (2021). Enhancing the storage and gastrointestinal passage viability of probiotic powder (Lactobacillus Plantarum) through encapsulation with pickering high internal phase emulsions stabilized with WPI-EGCG covalent conjugate nanoparticles. *Food Hydrocolloids, 116*, Article 106658. https://doi.org/10.1016/j.foodhyd.2021.106658

Ren, C., Xiong, W., Li, J., & Li, B. (2019). Comparison of binding interactions of cyanidin-3-O-glucoside to β-conglycinin and glycinin using multi-spectroscopic and thermodynamic methods. *Food Hydrocolloids, 92*, 155–162. https://doi.org/10.1016/j.foodhyd.2019.01.053

Ribeiro, E. F., Morell, P., Nicoletti, V. R., Quiles, A., & Hernando, I. (2021). Protein- and polysaccharide-based particles used for Pickering emulsion stabilisation. *Food Hydrocolloids, 119*, Article 106839. https://doi.org/10.1016/j.foodhyd.2021.106839

Shi, A., Feng, X., Wang, Q., & Adhikari, B. (2020). Pickering and high internal phase Pickering emulsions stabilized by protein-based particles: A review of synthesis, application and prospective. *Food Hydrocolloids, 109*, Article 106117. https://doi.org/10.1016/j.foodhyd.2020.106117

Shi, M., Wang, F., Jiang, H., Qian, W., Xie, Y., Wei, X., & Zhou, T. (2020). Effect of enzymatic degraded polysaccharides from Enteromorpha prolifera on the physical and oxidative stability of fish oil-in-water emulsions. *Food Chemistry, 322*, Article 126774. https://doi.org/10.1016/j.foodchem.2020.126774

Sui, X., Sun, H., Qi, B., Zhang, M., Li, Y., & Jiang, L. (2018). Functional and conformational changes to soy proteins accompanying anthocyanins: Focus on covalent and non-covalent interactions. *Food Chemistry, 245*, 871–878. https://doi.org/10.1016/j.foodchem.2017.11.090

Sun, Y., Zhong, M., Zhao, X., Li, Y., Qi, B., & Jiang, L. (2022). Stability and digestion characteristics of pickering high internal phase emulsions formed by acid-induced soy lipophilic protein, beta-conglycinin, and globulin. *Lwt-Food Science and Technology, 153*, Article 112554. https://doi.org/10.1016/j.lwt.2021.112554

Tang, C., Sun, X., & Foegeding, E. A. (2011). Modulation of physicochemical and conformational properties of kidney bean vicilin (phaseolin) by glycation with glucose: implications for structure-function relationships of legume vicilins. *Journal of Agricultural and Food Chemistry, 59*(18), 10114-10123. https://doi.org/ 10.1021/jf202517f.

Xu, W., Zheng, S., Sun, H., Ning, Y., Jia, Y., Luo, D., … Shah, B. R. (2021). Rheological behavior and microstructure of Pickering emulsions based on different concentrations of gliadin/sodium caseinate nanoparticles. *European Food Research and Technology, 247*(10), 2621–2633. https://doi.org/10.1007/s00217-021-03827-6

Xu, Y., Liu, T., & Tang, C. (2018). Novel pickering high internal phase emulsion gels stabilized solely by soy β-conglycinin. *Food Hydrocolloids, 88*, 21–30. https://doi.org/10.1016/j.foodhyd.2018.09.031

Xu, Y., Tang, C., Liu, T., & Liu, R. (2018). Ovalbumin as an outstanding pickering nanostabilizer for high internal phase emulsions. *Journal of Agricultural and Food Chemistry, 66*(33), 8795–8804. https://doi.org/10.1021/acs.jafc.8b02183

Zhang, Y., Zhao, M., Ning, Z., Yu, S., Tang, N., & Zhou, F. (2018). Development of a sono-assembled, bifunctional soy peptide nanoparticle for cellular delivery of hydrophobic active cargoes. *Journal of Agricultural and Food Chemistry, 66*(16), 4208–4218.

Zhou, F., Huang, X., Wu, Z., Yin, S., Zhu, J., Tang, C., & Yang, X. (2018). Fabrication of zein/pectin hybrid particles stabilized Pickering high internal phase emulsions (HIPEs) with robust and ordered interface architecture. *Journal of Agricultural and Food Chemistry, 66*(42), 11113-11123. https://doi.org/10.1021/acs.jafc.8b03714.

Zhu, C., Zhang, H., Huang, G., & Xiao, J. (2021). Whey protein isolate-low methoxyl pectin coacervates as a high internal phase Pickering emulsion stabilizer. *Journal of Dispersion Science and Technology, 42*(7), 1009–1020. https://doi.org/10.1080/01932691.2020.1724801

Zou, Y., Zhong, J., Pan, R., Wan, Z., Guo, J., Wang, J., … Yang, X. (2017). Zein/tannic acid complex nanoparticles-stabilised emulsion as a novel delivery system for controlled release of curcumin. *International Journal of Food Science and Technology, 52*(5), 1221–1228. https://doi.org/10.1111/ijfs.13380